2019

Effects of micro flexible rolling and annealing on microstructure, microhardness and texture of aluminium alloy

Mingshuai Huo
University of Wollongong, University of Science and Technology Liaoning, mh317@uowmail.edu.au

Jingwei Zhao
University of Wollongong, jzhao@uow.edu.au

Haibo Xie
University of Wollongong, xie@uow.edu.au

Fanghui Jia
University of Wollongong, fj910@uowmail.edu.au

Shengli Li
University of Science and Technology Liaoning

See next page for additional authors

Effects of micro flexible rolling and annealing on microstructure, microhardness and texture of aluminium alloy

Abstract

The microstructure and texture after plastic deformation are strongly dependent on the corresponding manufacturing process and subsequent annealing which significantly affect the properties of the final products. In this study, 1060 aluminium alloy with a thickness of 464 μm was micro flexibly rolled to a constant thickness ratio of 3.6 by a combined control of the roll gap, the rolling speed and the roll lifting speed. Afterwards, the rolled specimens were subjected to isochronal annealing at a temperature range of 200 to 400 °C for 30 min and isothermal annealing at 400 °C for 10-60 min. Results indicate that the microstructure, microhardness and texture of each thickness zone are distinctly influenced by the rolling parameters and annealing conditions. Specimens annealed at 400 °C for 30 min result in a relatively steady hardness distribution along the transition zones. Typical β fibre texture is observed in the specimens suffered from annealing while S is predominant in both micro flexibly rolled and annealed specimens.

Disciplines

Engineering | Science and Technology Studies

Publication Details

Huo, M., Zhao, J., Xie, H., Jia, F., Li, S., Zhang, H. & Jiang, Z. (2019). Effects of micro flexible rolling and annealing on microstructure, microhardness and texture of aluminium alloy. Materials Characterization, 148 142-155.

Authors

Mingshuai Huo, Jingwei Zhao, Haibo Xie, Fanghui Jia, Shengli Li, Hongmei Zhang, and Zhengyi Jiang

Abstract

The microstructure and texture after plastic deformation are strongly dependent on the corresponding manufacturing process and subsequent annealing which significantly affect the properties of the final products. In this study, 1060 aluminium alloy with a thickness of 464 μm was micro flexibly rolled to a constant thickness ratio of 3.6 by a combined control of the roll gap, the rolling speed and the roll lifting speed. Afterwards, the rolled specimens were subjected to isochronal annealing at a temperature range of 200 to 400 °C for 30 min and isothermal annealing at 400 °C for 10-60 min. Results indicate that the microstructure, microhardness and texture of each thickness zone are distinctly influenced by the rolling parameters and annealing conditions. Specimens annealed at 400 °C for 30 min result in a relatively steady hardness distribution along the transition zones. Typical β fibre texture is observed in the specimens suffered from annealing while S is predominant in both micro flexibly rolled and annealed specimens.

Keywords: Micro flexible rolling; Annealing; Microstructure; Microhardness; Texture; Aluminium alloy

1 Introduction

Thin materials with thickness less than one millimetre are widely used in the manufacturing of micro-parts which have extensive applications in the micro electromechanical systems and medical industry [1-8]. Thin strip with varying thicknesses fabricated by micro flexible rolling is a new kind of micro-parts, and have attracted a great interest. During micro flexible rolling, raw materials are formed with a periodical change of roll gap controlled by the pre-set PLC programs. Engler et al. [9] studied the flexible rolling processes of AA 5xxx and AA 6xxx-series aluminium alloys, and outlined that the whole processing chains of these two materials with a consideration of their special features such as the work hardening and age hardening. Qu et al. [10, 11] explored micro flexible rolling with a consideration of grained inhomogeneity using 3D Voronoi tessellation approach, and analysed the springback behaviour in the thickness direction of thin strip with varying thicknesses.

The evolution of microstructure and crystallographic textures of pure aluminium and aluminium alloys during flat rolling process has been a long term subject of research since it plays a vital part in semi- and final products' properties such as anisotropy, the strength, formability, ductility and drawability [12]. It is well known that, β fibre commonly dominates the texture development in face-centred cubic (FCC) metals after cold rolling (plane strain state) [13, 14]. This typical rolling texture is epitomised by a continuous tube of orientations which rotate from the Copper orientation {112}<111> through the S orientation {123}<634> to the Brass orientation {011}<211> [15, 16]. Yuan et al. [17] investigated the influences of grain shape on the texture development of AA 5754 aluminium alloys after cold rolling, and found that the elongated grains in the rolling direction preferred to rotate to the β fibre under flat rolling than that under cross rolling. In addition, heating rate plays a significant role in the properties of final products due to different precipitations from various recrystallisaiton processes [18]. Xia et al. [19] examined the dependence of heating rate on microstructure, texture and mechanical properties of AA 5083 aluminium alloy, and the results indicated that the heating rate affected significantly the recrystallised microstructure and texture, and the Cube {001}<100> orientation favoured to be formed in the fine equiaxed grains in the case of rapid annealing. Rolling geometry is also of importance in mechanical properties, microstructure and texture evolution [20-23]. Major [24] carried out experimental work in order to clarify the variations of microstructure, texture and stored energy by differing the l/h ratios (l is the projected roll arc length, and h represents the average thickness of the specimen). The results disclosed that shear texture existed in the surface layers in the case of high l/h ratio, and for the medium l/h rate case, specimens with rolling texture displayed much higher extent of stored energy than that with shear texture.

Chemical compositions and precipitates affect significantly the microstructure and texture of the alloys under the conditions of both deformation and annealing [25]. Lücke et al. [26] observed the formation of severe shear bands in the sheared particles, resulting into the noticeable planar slips. In this case, intense Goss {011}<100> and Brass orientations were developed when fine particles restricted the shear bands into only one or few grains. Comparatively, non-shear particles such as coarse particles gave a rise to the occurrence of deformation area close to the particles due to massive pile-ups of dislocations. In addition, Engler et al. [27] studied the impact of composition on the microstructure and texture within five kinds of alloys. They stated that both of rising strength and bigger grain size expedited the shear behaviour which led to the generation of greater amount of Brass orientation on the behalf of consumed Copper and S orientations. Liu et al. [28, 29] developed a model to predict the texture development during cold rolling by quantifying the texture volume fractions and true rolling strains. They concluded that the higher strain hardening resulted from deformation procedures led to the impediment of the lattice rotation from the initial orientations to the β fibre orientations, then affecting the generation of rolling textures.

Although extensive scholars have investigated the microstructure and texture in flat rolling of the products with constant thickness distribution, few studies have been conducted on the thin strip with varying thicknesses along the longitudinal direction. The current investigation aims to study the microstructural evolution and texture development of thin strip with varying thicknesses produced by micro flexible rolling and subsequent annealing processes, and the deformation features are discussed clearly.

2 Materials and experimental setup

1060 aluminium alloy with a thickness of 464 μm was used in this study. Its chemical compositions are given in Table 1. Specimens were cut into 150 × 15 mm^2 and subjected to a full recrystallisation solution treatment at 500 °C for 2 h. The heat-treated specimens were then micro flexibly rolled to varying thicknesses with a constant thickness ratio (the ratio of thickness at thicker zone to that of thinner zone) of 3.6. The rolling schedule is presented in Table 2. The rolls' diameter and barrel length are 25 and 40 mm, respectively.

Table 1 Chemical composition (wt.%) of the investigated alloy.

Si	Fe	Ti	Al	Others
0.08	0.26	0.013	99.61	0.037

Table 2 Micro flexible rolling schedule.

Rolling parameter	Value
Initial thickness (μm)	464
Thickness at thicker zone (μm)	346
Reduction at thicker zone (%)	25.4
Thickness at thinner zone (μm)	96
Reduction at thinner zone (%)	79.3
Thickness ratio	3.60
Rolling speed (cm/min)	60

The setup of micro flexible rolling process is shown in Fig. 1. The whole rolling procedure is controlled by PLC programs. Micro flexible rolling starts when the dragging force generates from the rotation of rolls. With the progress of rolling, the lifting speed interferes gradually in accordance with the pre-set program. Afterwards, a thickness transition zone with a slope will be obtained, depending on the combination of the rolling speed, the lifting speed and the work hardening behaviour of the specimens being rolled.

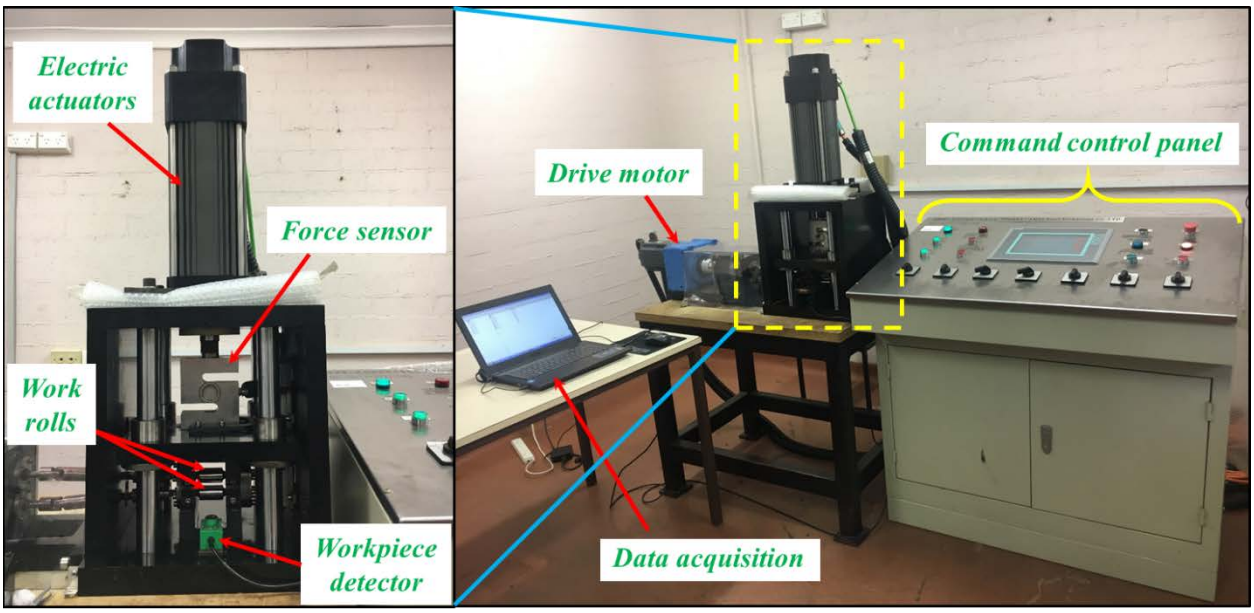

Fig. 1. Sketched illustration of micro flexible rolling system.

Two kinds of heat treatment processes, including isochronal and isothermal annealing, were performed on micro flexibly rolled strip. The details of the heat treatment process are shown in Fig. 2. For the isochronal treatment, specimens were annealed for 30 min at 200, 300 and 400 °C. For the isothermal treatment, specimens were annealed at 400 °C for 10, 30 and 60 min. Water quenching was immediately applied to all the specimens after annealing.

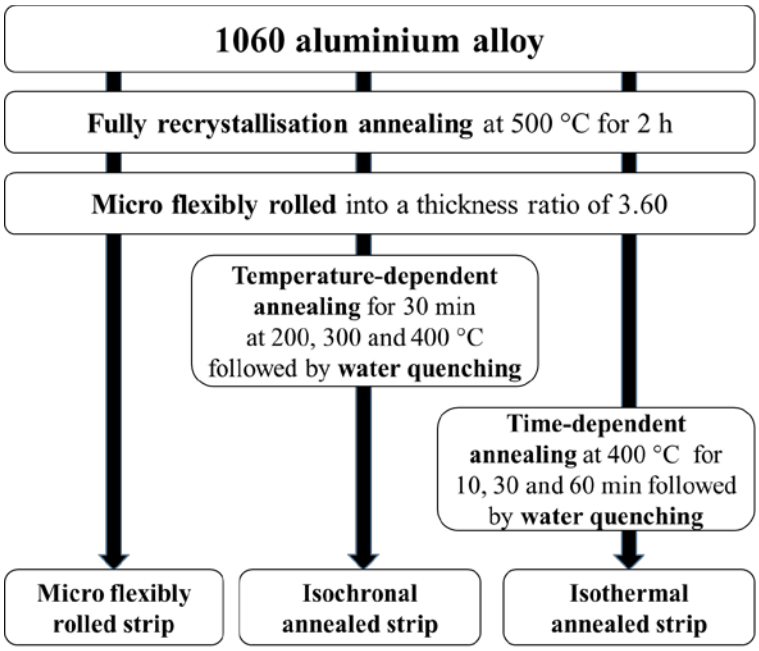

Fig. 2. Heat treatment processes of the thin strip with varying thicknesses.

The locations for microstructural observation and microhardness testing of the specimens are labelled in Fig. 3. Electrolytic etching for microstructural observation was performed on the Struers Lectropol® 5 electrolytic polishing/etching unit. Barker's reagent was used as etchant with the etching time of 10-15 s and voltage of 24 V. Subsequently, Leica DMRM and Nikon Fluorescence Microscope were used for the identification and acquisition of the polarised light false colour optical micrographs from cross-sections as defined by the rolling direction (RD) and the normal direction (ND). Vickers microhardness was tested by a TIME TH715 microhardness tester along the cross-sections after polishing. Five independent positions were selected from the thicker zone to the thinner zone (as shown in Fig. 3), with a load of 0.49 kgf and a dwelling time of 10 s.

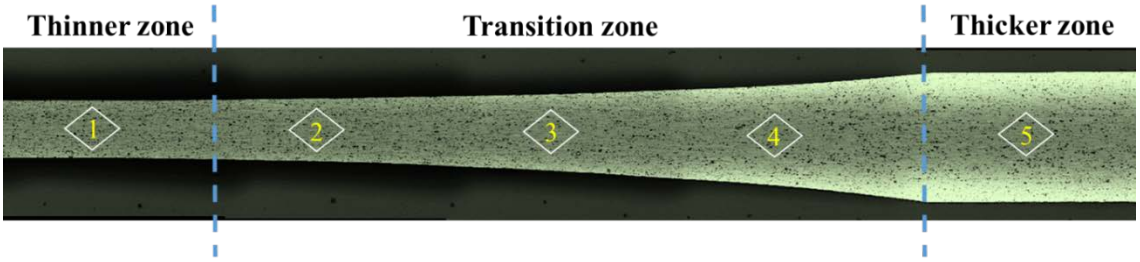

Fig. 3. Measured positions of microhardness in the thicker, transition and thinner zones.

Electron back-scattering diffraction (EBSD) was performed on a JEOL® JSM-7001F field emission gun-scanning electron microscope (FEG-SEM) using the Oxford Instruments Corona Fast Acquisition software. Post-processing of the measured maps was performed using the HKL-Channel 5 software. For the analysis of microtexture, the orientations were expressed in the form of a set of Euler angles ($\varphi_1, \varphi, \varphi_2$). Orientation distribution function (ODF) sections were computed using Bunge's notation in view of specimens' orthorhombic symmetry.

3 Results

3.1 Microstructure and microhardness

Fig. 4 shows the microstructure and microtexture of aluminium strips heat-treated at 500 °C for 2h. It can be seen from Fig. 4(a) that homogeneously equiaxed and polygonal grains with an average grain size of 30 μm have been obtained. The initial texture is dominated by typically recrystallised Cube orientation, as shown in Fig. 4(b).

The microstructure of the thin strip after micro flexible rolling is shown in Fig. 5. It can be seen that a visually flattened phenomenon of the grains is observed throughout the thickness direction of the specimens even though only a slight reduction acted on the thicker zone. Contrarily, extremely deformed grains with waved characteristics are observed in the thinner zone due to high rolling reduction, resulting in a heavy plane strain. This phenomenon frequently happens in the cold rolled strip with intermediate strains.

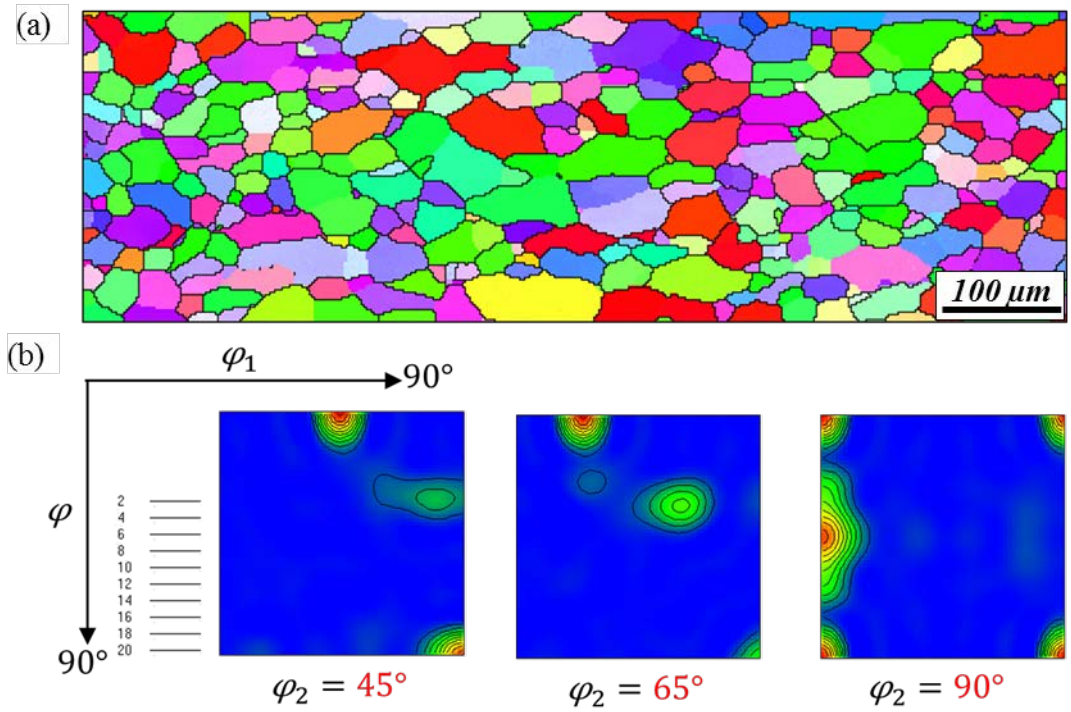

Fig. 4. Aluminium strip heat-treated at 500 °C for 2h: (a) microstructure, and (b) texture.

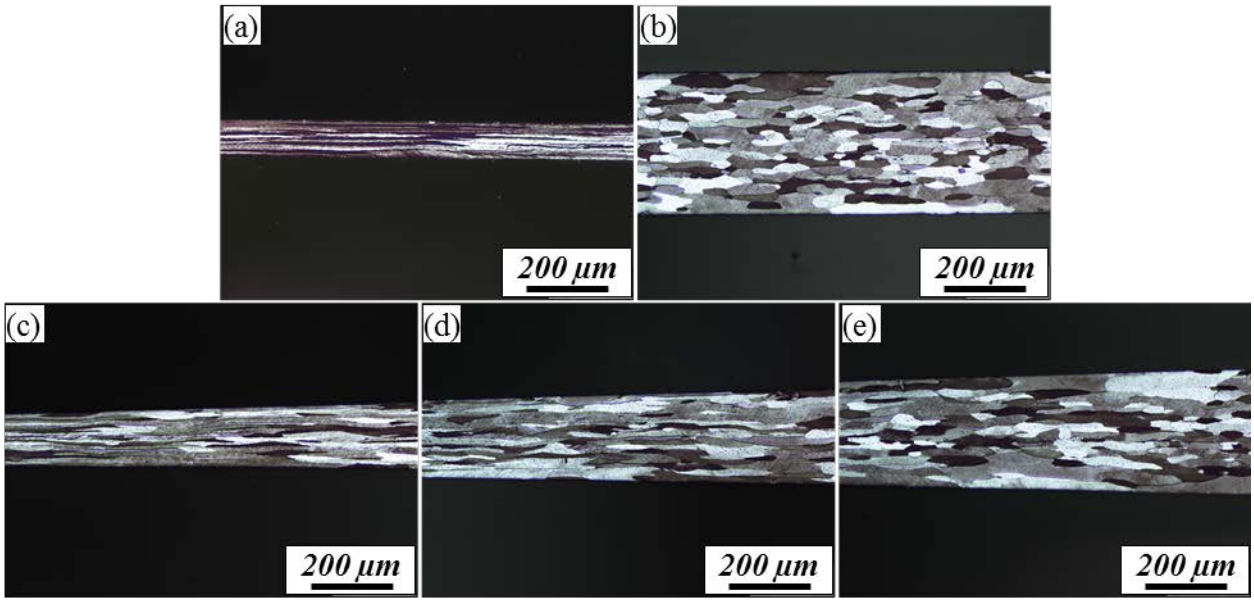

Fig. 5. Microstructure of the strip after micro flexible rolling in the (a) thinner, (b) thicker and (c-e) transition zones.

Fig. 6 shows the microstructural comparison of the thinner zones between after isochronal annealing and isothermal annealing. It can be seen that waved grains with enormously elongated phenomenon exist after isochronal annealing at 200 °C for 30 min, as shown in Fig. 6(a). At a higher annealing temperature of 300 °C, more flattened grains form, and the grain boundaries are nearly aligned to the rolling direction.

This suggests that the recovery has occurred during annealing treatment. When the annealing temperature reaches 400 °C, recrystallisation phenomenon takes place, and fine grains are found in the central layer (Fig. 6(c)). For the isothermally annealed specimen at 400 °C for 10 min, elongated grains without waved characteristics are found. However, the specimens annealed at 400 °C for both 30 and 60 min display the recrystallisation behaviour. By contrast, coarse grains are found to distribute homogenously in the specimen with the holding time of 60 min.

Fig. 7 compares the microstructure in the thicker zones after two annealing procedures. It can be found that the microstructure in the thicker zones is not sensitive to temperature, with no recrystallisation, when the holding time is 30 min. The specimen subjected to the annealing at 400 °C for 60 min is the only one which presents the recrystallisation phenomenon with the obvious inhomogeneous grain size.

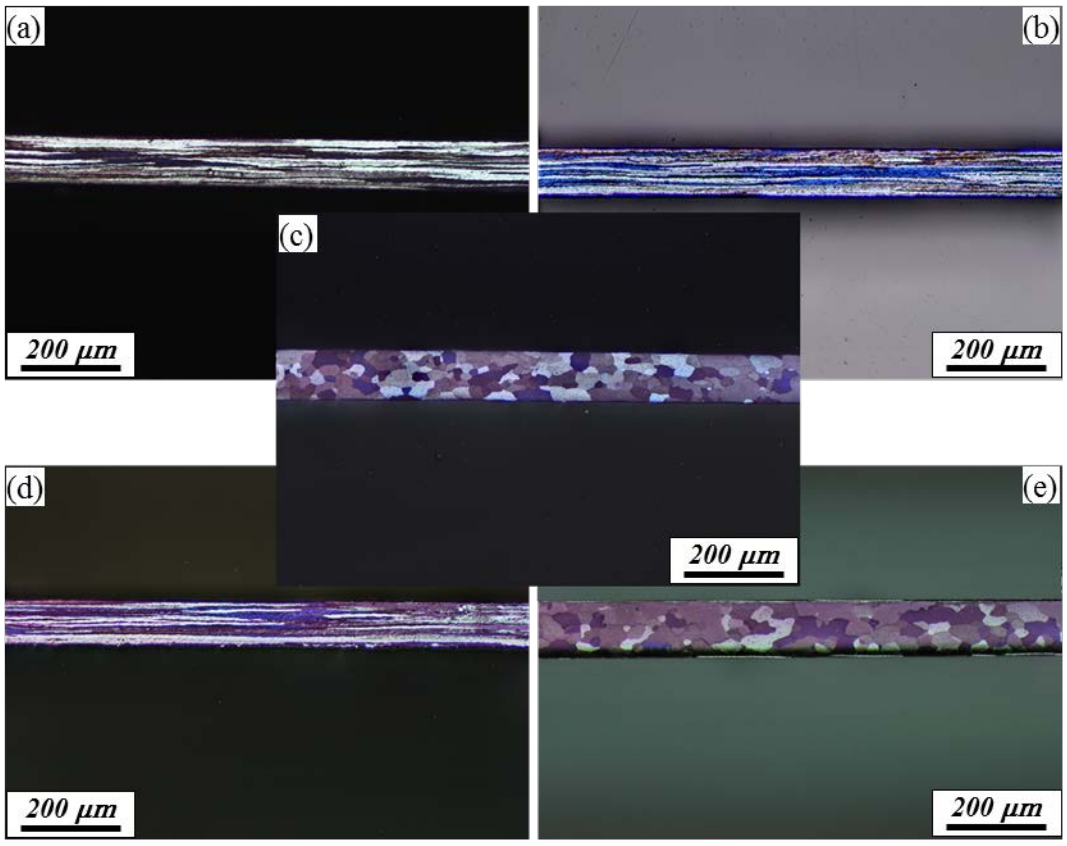

Fig. 6. Microstructure of the thinner zones after isochronal annealing at (a) 200 °C, (b) 300 °C, (c) 400 °C for 30 min, and isothermal annealing at 400 °C for (d) 10 min and (e) 60 min.

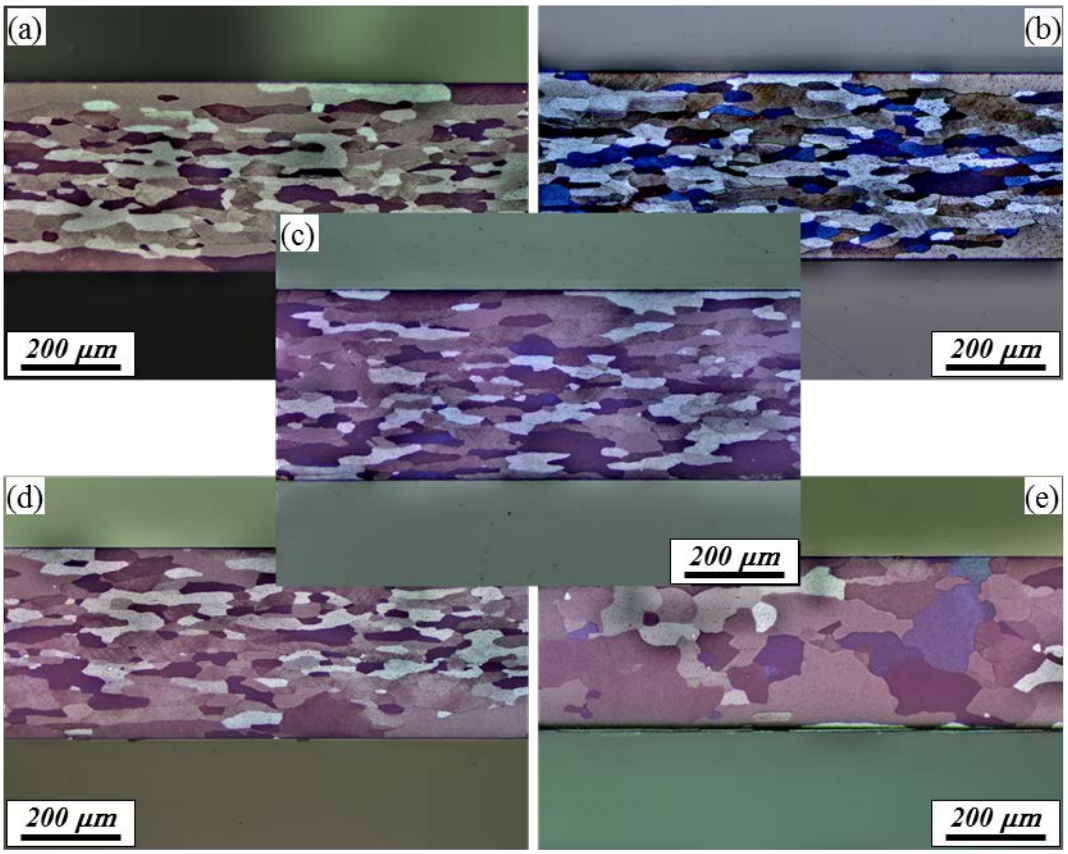

Fig. 7. Microstructure of the thicker zones after isochronal annealing at (a) 200 °C, (b) 300 °C, (c) 400 °C for 30 min, and isothermal annealing at 400 °C for (d) 10 min and (e) 60 min.

Fig. 8 shows the variation of microstructure in the transition zones after isochronal annealing or isothermal annealing. Similar to the thinner zones, no recrystallisation takes place in the specimens annealed at 200 and 300 °C. The waved phenomenon of deformed grains is observed in the transition zones close to the thinner zones, and disappears progressively with the decrease of reduction. Meanwhile, the spacing of the grain boundaries shifts based on the change of the reduction acting on the corresponding thickness zone. Differently, specimen annealed at 400 °C displays full recrystallisation in former two portions (Fig. 8g and h). The recrystallisation, however, seems to be terminated in the transition zone where approaches to the thicker zone. This means that higher rolling reduction will give a comparative edge in providing energy for annealing. That is also the reason why there is no recrystallisation phenomenon being observed in the thicker zone, as shown in Fig. 7(e). For the specimen under isothermal annealing at 400 °C for 10 min, even though with a short holding time the grains become much stretched compared to the waved morphology of the microstructure after micro flexible rolling. However, there is no recrystallisation occurring in all the three portions. By contrast, full recrystallisation phenomenon can be found in the

specimens with the holding time higher than 30 min. Evidently, finer grains emerge normally in the central layer rather than in the surface layers.

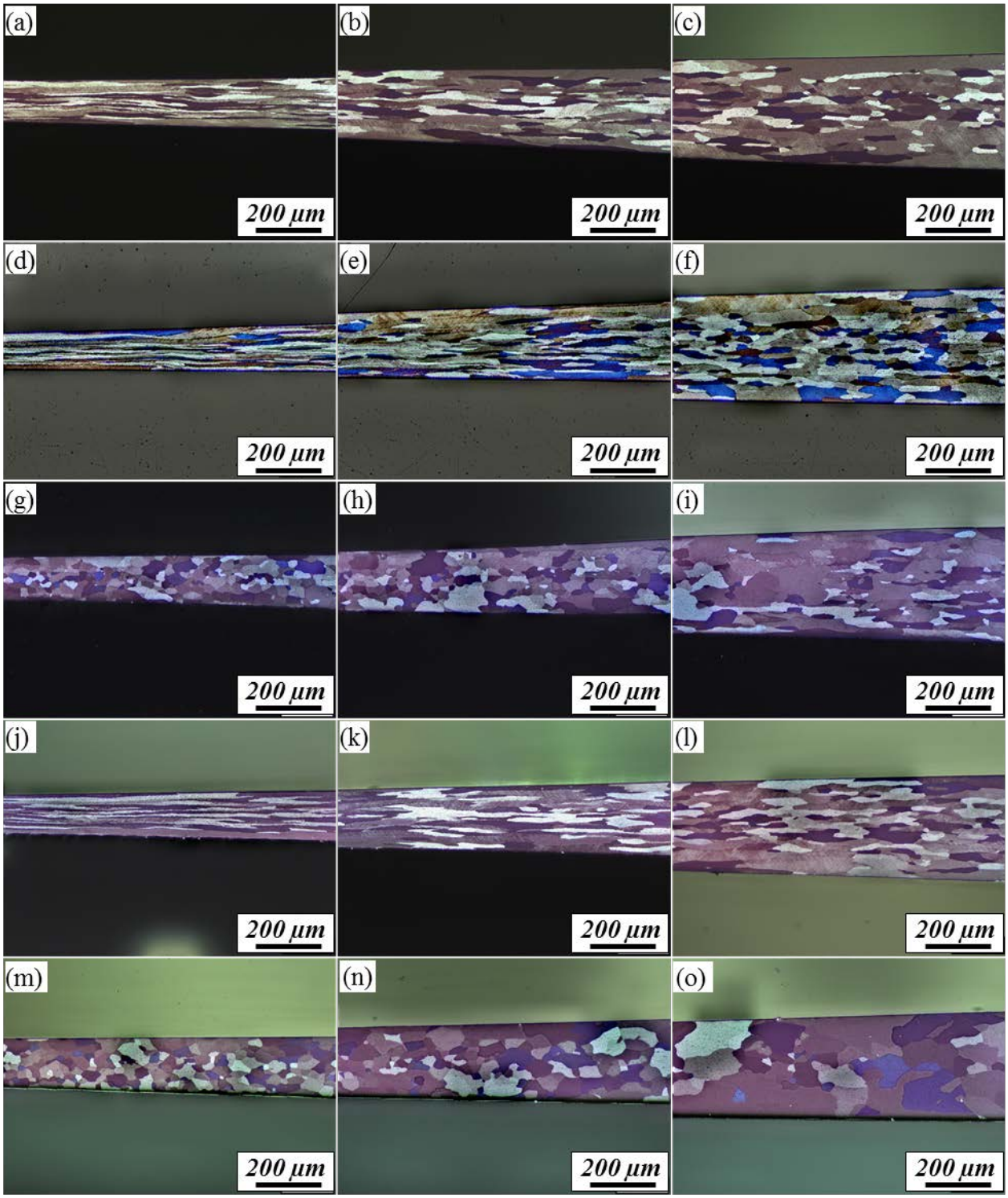

Fig. 8. Microstructure of the transition zones after isochronal annealing at (a-c) 200 °C, (d-f) 300 °C, (g-i) 400 °C for 30 min, and after isothermal annealing at 400 °C for (j-l) 10 min and (m-o) 60 min.

Microhardness of the micro flexibly rolled and annealed strips from the thinner to thicker zones along the rolling direction is illustrated in Fig. 9. It can be found that thinner zones with the larger rolling reduction exhibit comparatively higher microhardness, and drop steadily to the lower values in the thicker zones with the smaller rolling reduction. Meanwhile, microhardness of micro flexibly rolled strip in each measured position presents the highest values in all cases. After annealing, different degrees of softening behaviour can be found depending on the annealing temperature, the annealing holding time and the rolling reductions. For the isochronal annealing case, microhardness gradually decreases with increasing the annealing temperature from 200 to 400 °C. It is worthy to note that the microhardness in the specimen annealed at 400 °C indicates a much gentle variation along the rolling direction. For the isothermal annealing at 400 °C with different holding times, only a slight drop is observed in the specimen with 10 min holding time compared to the micro flexibly rolled strip. When the holding time exceeds 30 min, an explicit decrease can be found in all measured positions. These microhardness results are highly consistent with the examinations of the microstructure evolution in the previous context.

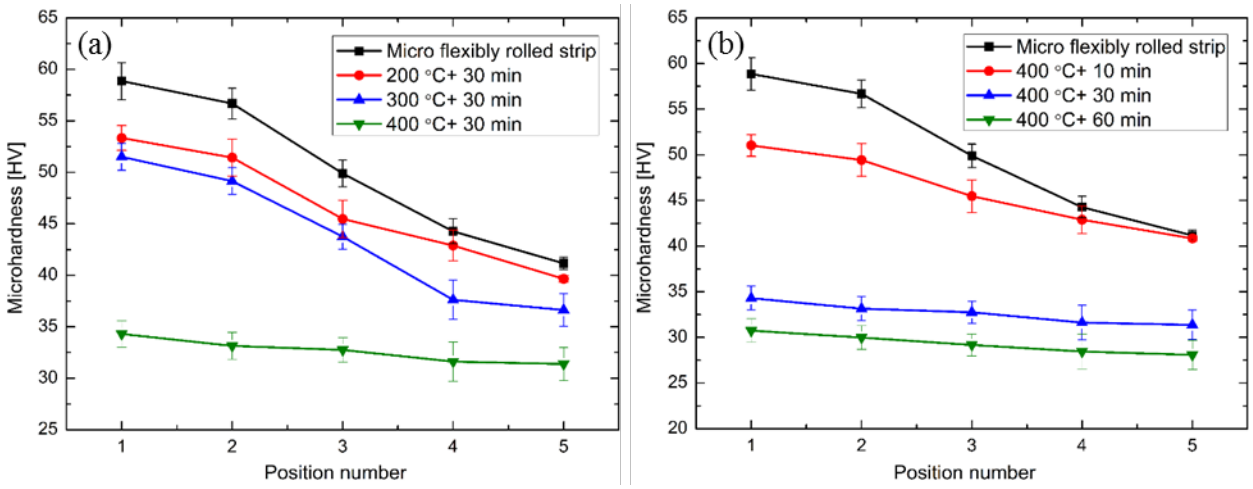

Fig. 9. Variations of Vickers hardness of strips after micro flexibly rolling vs. (a) isochronal annealing, and (b) isothermal annealing in five measured positions.

3.2 Texture

Transition zone plays a dominant role in thin strip with varying thicknesses since its gradational structure connects the utmost crest and least trough of various thickness zones, which determines the most characteristics especially of mechanical properties. In order to characterise the texture evolution in the transition zone, EBSD mappings were conducted in three specified portions of the specimens after micro flexible rolling and subsequent annealing, which almost cover the whole transition zones, as shown in Figs. 10 and 12.

Fig. 10 shows the inverse pole figure maps of the micro flexibly rolled specimen in three specified portions (MFR1-MFR3) of the transition zone. It can be found that grains in the central layers nearly parallel to the rolling direction, in which most of them favour to rotate near the <101> direction. While the grains in the surfaces layers tend to deform aligned to the rolling paths which prefer to rotate close to the <001> or <111> directions. In contrast, grains in all layers deformed severely gradually from the MFR3 to MFR1 portions, which are related to the strain rate acting on the corresponding portion. Consequently, the most elongated grains are found in MFR1 with the smallest spacing of the grain boundaries.

Owing to the most significant features of rolling textures concentrate in the φ_2 sections, sections of φ_2 at 45, 65 and 90° from the complete ODFs are used to clarify the effect of micro flexible rolling and subsequent annealing on the texture development. Fig. 11 shows the texture of MFR1-MFR3 portions with φ_2 sections of ODFs. It covers the range of typically encountered textures in FCC metals after plane strain deformation. The initial texture gradually rotates to the β fibre textures which extend through the orientation space from near Copper orientation to S orientation then to Brass orientation in all the ODFs results. With the increase of rolling reduction, the intensity of cube orientation drops, whereas an increase tendency raises in the strength of β fibre rolling textures as well as the Goss orientation.

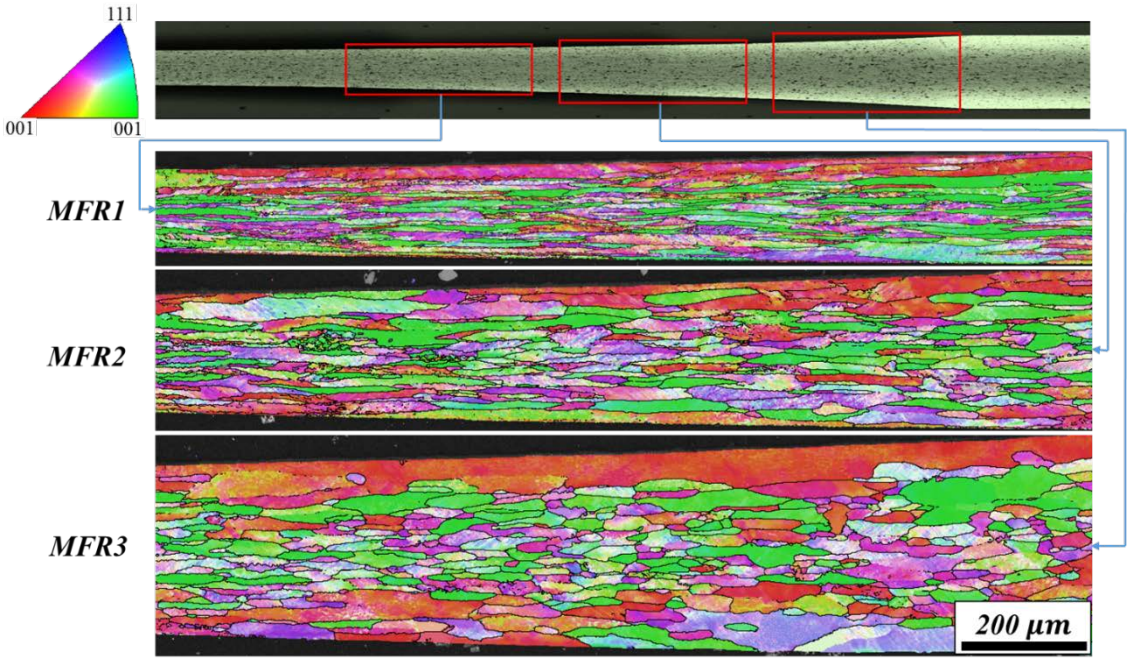

Fig. 10. Inverse pole figure maps of the micro flexibly rolled specimen in three specified portions along the transition zone.

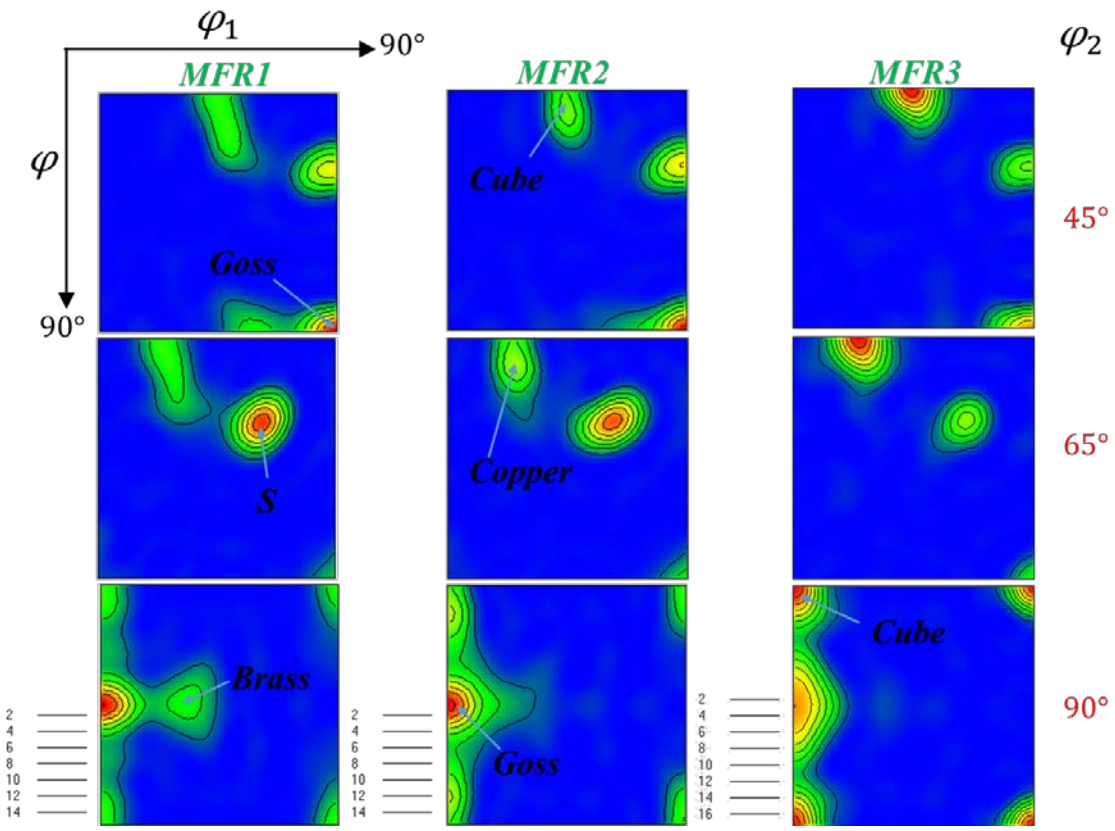

Fig. 11. Orientation distribution functions (ODFs) of the micro flexibly rolled specimen in three specified portions along the transition zone and directions at $\varphi_2 = 45°, 65°$ and 90°.

Fig. 12 shows the inverse pole figure maps of the specimen annealed at 400 °C for 30 min in three specified portions (A1-A3) along the transition zone. It can be seen that much finer grains are observed in the central layer of A1 and A2 portions than those in the surface layers. They prefer to rotate to a random distribution of directions. For the A3 portion, however, recrystallisation mostly occurs in the central layer, and coarse grains are observed in the region with lower deformation strain. Meanwhile, many adjacent grains in the surface layers are still in elongated state with few recrystallisation. Also, most grains in the central layer prefer to rotate near the <101> direction, which is rather analogous to results from the flexibly rolled portions (MFR1-MFR3).

Fig. 13 gives the texture of A1-A3 portions with φ_2 sections of ODFs. It can be found that the rolling texture of β fibre become much weaker in A1 and A2 portions after annealing at 400 °C for 30 min. Alternatively, Cube orientation occupies the dominant position with the relatively higher peak intensity. In contrast, the texture in the A3 portion still displays a feature of rolling texture. The most likely reason is due to the occurrence of deformed grains observed in the corresponding portion (A3).

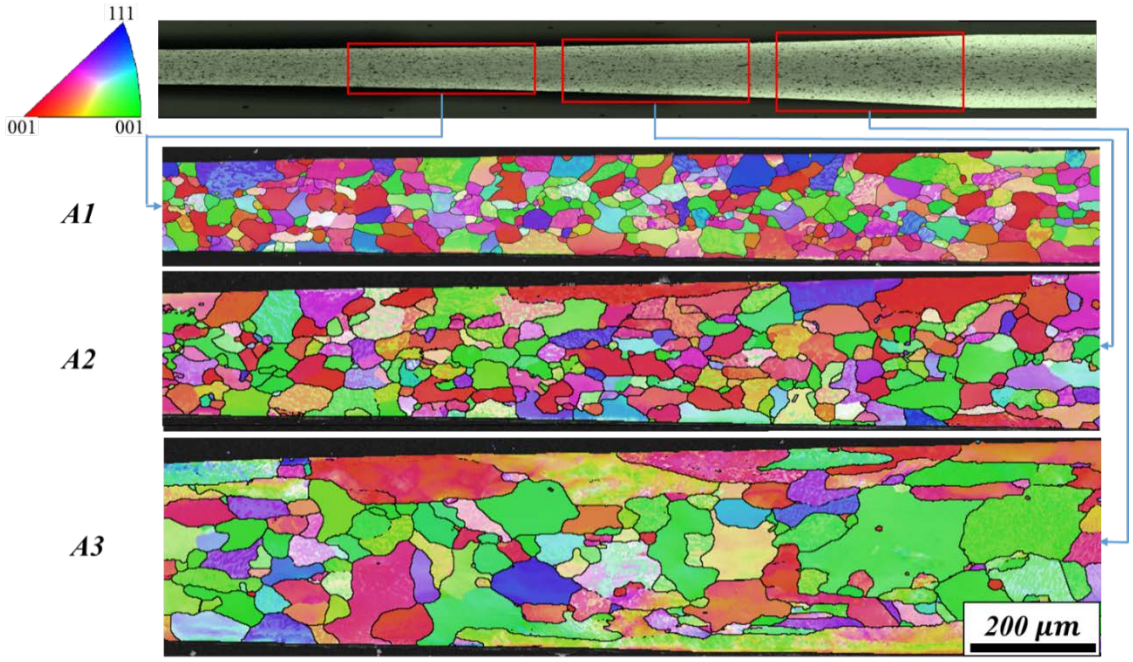

Fig. 12. Inverse pole figure maps of the specimen annealed at 400°C for 30 min in three specified portions along the transition zone.

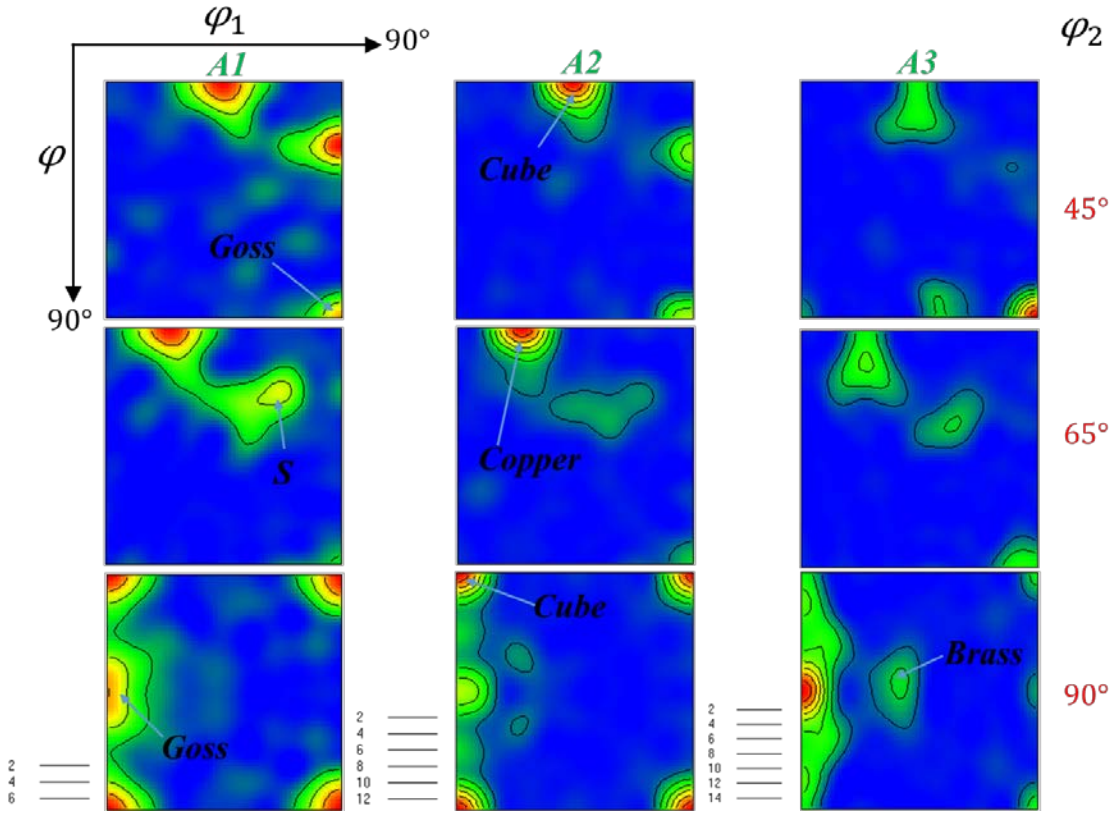

Fig. 13. Orientation distribution functions (ODFs) of the specimen annealed at 400°C for 30 min in three specified portions along the transition zone and directions at $\varphi_2 = 45°, 65°$ and $90°$.

Fig. 14 shows the comparison of misorientations in the three specified portions of the micro flexibly rolled and subsequent annealed specimens. It can be seen that there are a large number of low angle grain boundaries (LAGBs) in the micro flexibly rolled portions (Fig. 14a-c). The slipping of plastic deformation leads to the increase of dislocations which will result in the emergence of subgrains. In addition, MFR1 with the highest deformation rate obtains the biggest volume fraction (34.96%) of high angle grain boundaries (HAGBs) and gradually decreases to 30.12% at MFR3 with relatively low reduction ratio. After annealing at 400 °C for 30 min, the percentage of HAGBs in each annealed portion (A1-A3) presents a big boost. Similar to the micro flexibly rolled portions, the annealed ones also display a degressive tendency from the A1 to A3 portion even though the variations are not remarkable.

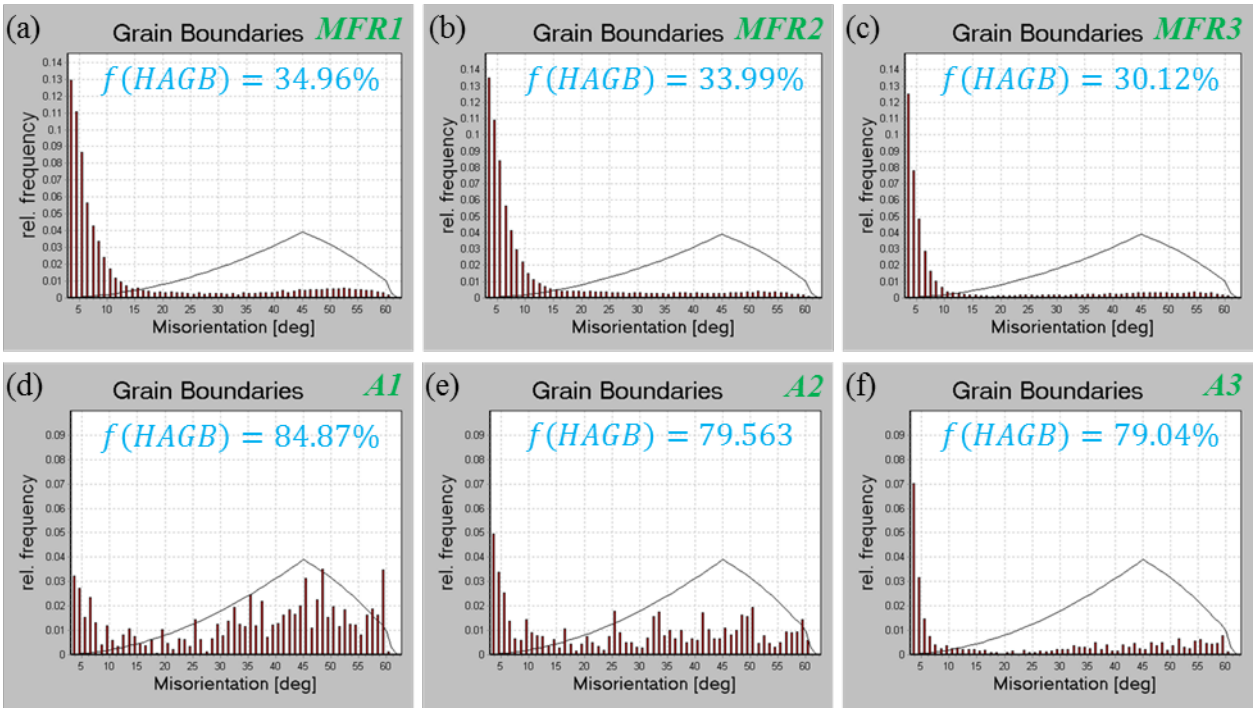

Fig. 14. Misorientation variation of the (a-c) micro flexibly rolled specimens, and (d-f) recrystallised specimens at 400°C for 30 min in three specified portions along the transition zone.

The volume fraction variations of the major textures after micro flexible rolling and subsequent annealing in the three specified portions are shown in Fig. 15. It can be found that S (R) orientation occupies the highest percentage in all the portions no matter in the micro flexibly rolled and annealed specimens. For the micro flexibly rolled one, the strength of S and Goss orientations raise with the increase of deformation rate. Differently, all the Cube, Brass and Copper orientations present a decrease trend. Following the annealing at 400 °C for 30 min, the volume fractions of almost all the orientations in A1-A3 portions have dropped compared with that in the MFR1-MFR3 portions. Among them, S orientation's strength drops sharply in A1 and A2 portions while only a few decrease is measured in the A3 portion. In addition, Goss,

Brass and Copper orientations show the contrary variation tendency compared with the measured portions in the micro flexibly rolled ones. It is worth to note that an increasing trend occurs in Cube orientation during A1 and A2 portions. However, there is a big reduction of volume fraction in A3 portion.

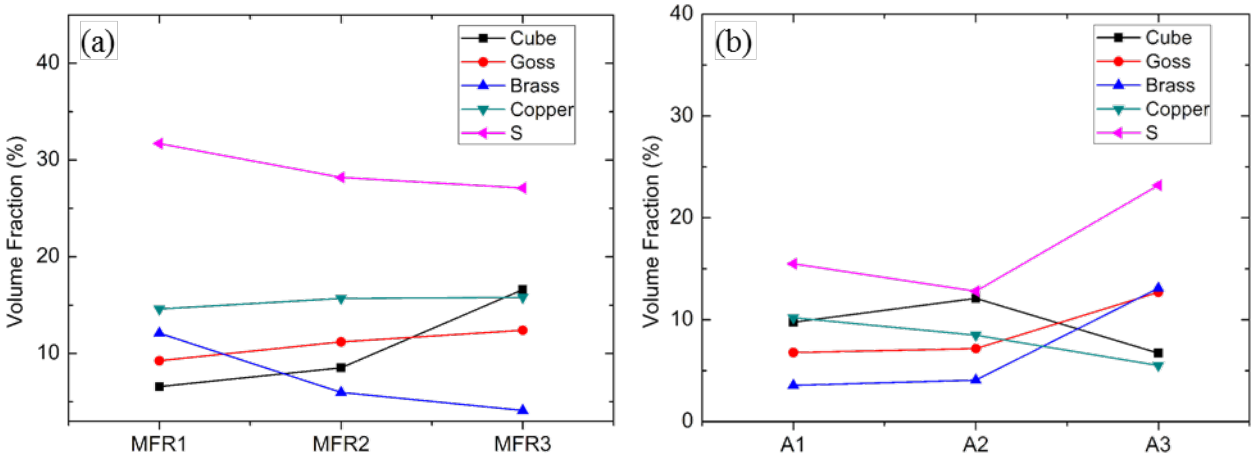

Fig. 15. Volume fraction variations of textures in three specified portions along the transition zone in (a) micro flexibly rolled specimen, and (b) recrystallised specimen at 400 °C for 30 min.

4 Discussion

4.1 Microstructural evolution and microhardness variation

The microstructural evolution along the transition zone is divided into three specified portions which represent the relatively low, intermediate and high reduction regimes, respectively. Inhomogeneous microstructural distribution is observed, and deformed grains with a higher rolling reduction have resulted in a higher volume fraction of HAGBs. This suggests that the ratio of HAGBs increases with increasing the strain while it will become much gentle once exceeds the critical strain [30]. Hansen et al. [31-34] found that high strain deformation in aluminium promote the emergence of subgrain boundaries. They pointed out that increasing strain led to an increase of the grain boundary area for a deformed polycrystalline metal. The characteristics of these boundaries are closely related to the flow stress, anisotropy and the corresponding recrystallisation behaviour [35]. For the current study, the grain spacing S_G in the normal direction can be evaluated using Eq. (1) [36]. With the same initial heat treatment condition, the initial grain size of each specimen G_0 is identical. Thus the increase of strain will directly lead to a decrease in the spacing of the HAGBs. In this case, the spacing of the HAGBs diminishes gradually from the MFR1 to the MFR3 portions (as shown in Fig. 10).

$$S_G = G_0 \exp(-\varepsilon) \tag{1}$$

where ε is the strain, and G_0 is the initial grain size.

An in-depth analysis about the MFR1 portion is shown in Fig. 16. The principal difference to the other two micro flexibly rolled portions (MFR2 and MFR3) is the significantly waved characteristics found in the central layer. This feature was frequently found both in single crystals with diverging texture orientations [37] and polycrystals with coarse grains [38]. Normally, various deformation bands could be observed in relatively coarse grains [26], which were frequently tilted to the rolling plane with approximately $\pm 35°$ and generated by minor dislocation cells with the rather high misorientation traversing the cell walls [39]. These are highly accordance with the comparison of misorientation profiles (as shown in Fig. 16) between the grains with and without obvious deformation bands, in which relatively larger difference of lattice misorientation was observed. Additionally, these heterogeneous deformation features of the grain subdivision presented more pronounced in the pure aluminium with medium or high deformation rate [40] and were designated with 'Copper type' shear bands associated to the local softening in matrix.

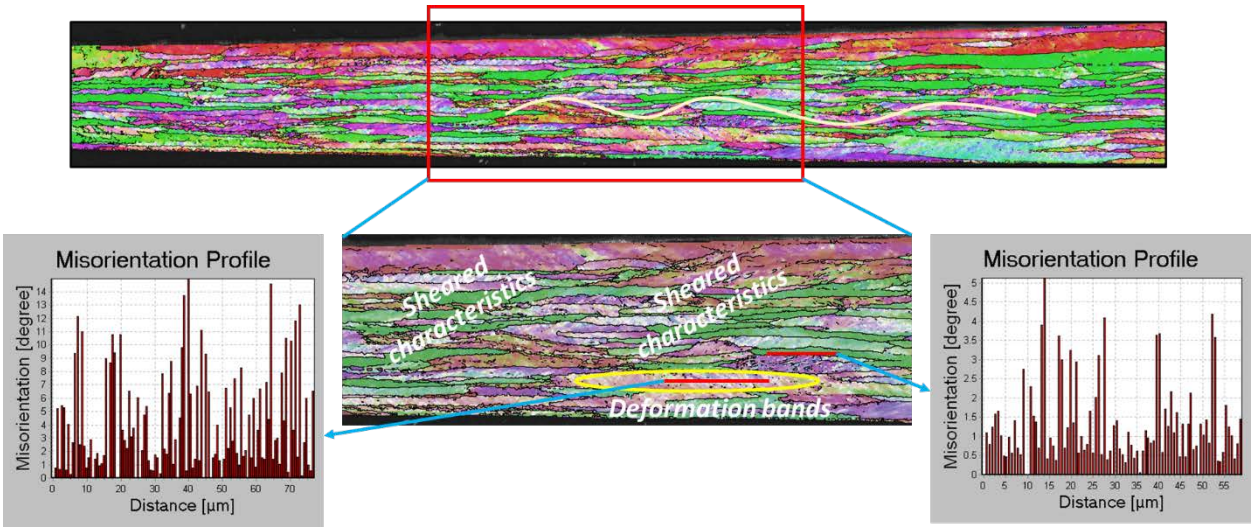

Fig. 16. Specific illustration of shear characteristics and misorientation comparison between the grains with and without deformation bands.

Isothermal and isochronal annealing processes have influenced significantly the microstructural distribution from the thinner to the thicker zones. The specimens annealed at temperature below 300 °C with 30 min holding time cannot obtain sufficient driving force for recrystallisation. Nevertheless, the microhardness values of the 200 and 300 °C specimens have somewhat decreased comparing to the micro flexibly rolled specimen, which means recovery has occurred. On raising the temperature to 400 °C, the recrystallised microstructure has been observed with inhomogeneous distribution of grain size in the various thickness zones. Note that finer grains always emerge in the central layer of the transition zone (Fig. 12)

while much coarser grains can be found in the surface layers. The reason about this can be understood through the mechanism sketched as shown in Fig. 17. During micro flexible rolling with the upward rolling process, the final contact forces of the roll arc area will have continuously a bearing on the interior evolution of microstructure. In terms of the stresses equilibrium on the transition zone, the resultant stress is therefore the combination of the interface pressures and the frictional forces which acted on the surface of the specimen. It has a close relationship with the variation of internal stress σ as expressed in Eq. (2) [41, 42] and parallel to the rolling plane in the central layer. Simultaneously, the direction of the frictional force is also continually changed which strongly depends on the forward slip and backward slip between the roll arc bite. This suggests that the resultant stress concentrated in the central layer will result in a relative motion between the central layer and the surface layers then lead to the shear phenomenon. Accordingly, the shear behaviour between different thickness layers will promote the inhomogeneous deformation features. In this case, it is supposed that the grains in the central layer can generate more nucleation sites in order to form much finer grains during recrystallisation, which coincides to the results of the microstructural evolution in Figs. 6 and 8.

$$l\frac{d\sigma}{di}+(\sigma+p)\left(\frac{dl}{di}+\gamma_1\frac{v_j}{v_i}\right)-2\gamma_2 q=0 \tag{2}$$

where l is the thickness of the specimen, σ is the longitudinal tensile stress of the strip, p is the normal pressure between the strip and work rolls, V_j is the vertical roll lifting speed, and V_i is the rolling speed of the specimen at point i. The value of γ_1 is 1 in the upward rolling and -1 in the downward rolling. $\gamma_2 q$ is the shear stress which is assumed by the well-known Coulomb's model $\gamma_2 \mu p$. Positive sign of γ_2 is used for backward slip zone and negative sign is for the forward slip zone. Compared to the average grain size in A1 and A2 portions which is continuously shifted to lager magnitude portions, it is pertinent to note that the phenomenon of inhomogeneous distribution without full recrystallisation is shown in A3 portion of Fig. 12. This phenomenon has led to the maintenance of most typical features from the deformed state, which normally occurred in the materials with a strong texture [43]. As shown in Fig. 14, few HAGBs in this portion resulting into a relatively low mobility should be another reason to explain about this. In addition, due to most of the stresses are localised in the central layer discussed in previous context, the stored energy obtained from deformation in the surface layers are almost released during the very early period of annealing and cannot supply the recrystallisation anymore. Thus the shape of grains in the surface layers still reveals the elongated shapes after micro flexible rolling while extremely coarse grains can be found in the central layer (as shown in the A3 portion of Fig. 12). Similar orientation characterisation among the deformed grains near surface layer resulted from the strong shear characterisation can be a reason leading to this phenomenon.

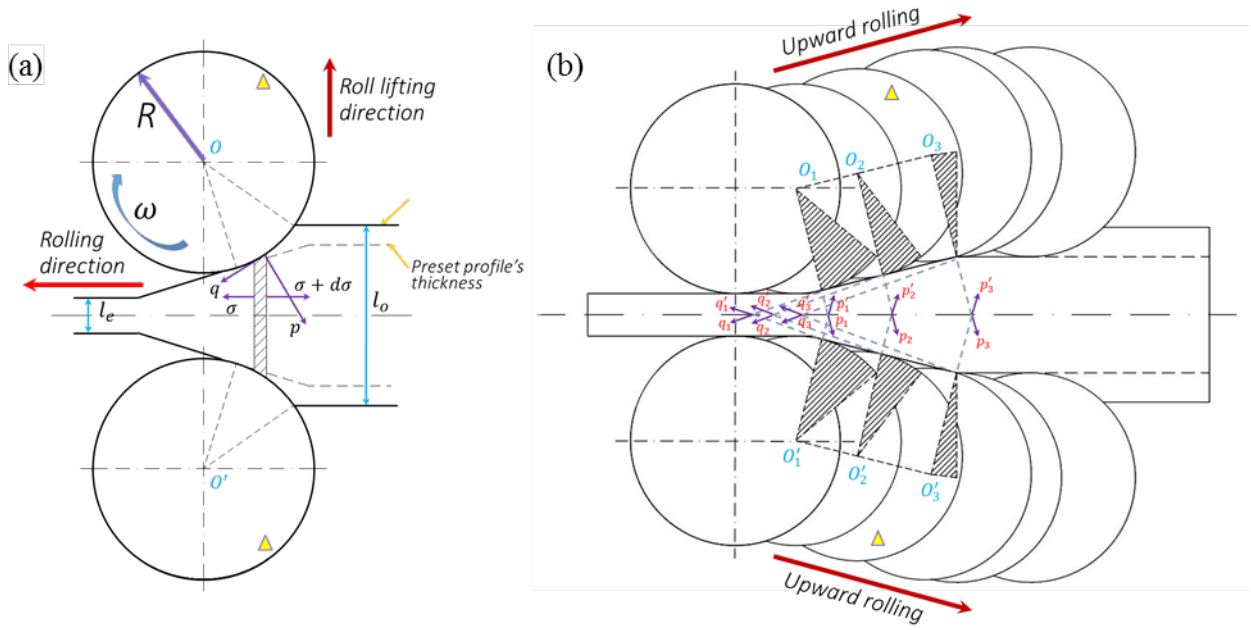

Fig. 17. Schematic illustration of (a) stress analysis in micro flexible rolling process, and (b) roll contact arc evolution and corresponding stresses distribution in different micro flexible rolling stages of upward rolling procedure.

4.2 Texture evolution

After micro flexible rolling, specimens in all the portions (MFR1-MFR3) exhibit typical FCC rolling textures (β fibre). Among them, S orientation dominates in all characteristic texture orientations and tends to increase the intensity with the growing of deformation strains from the portion MFR3 to MFR1 (as shown in Fig. 18). Meanwhile, its distribution mainly concentrates on the central layer, which is most likely related to the special deformation mechanism of shear characteristics discussed in previous context. Similar evolution trend has also occurred in Brass orientation. By contrast, a completely contradicted development can be found in the variation of Copper orientation. Engler et al. [44] has explained that the increase of Copper orientation is understood based on the consumption of Brass orientation. Additionally, although the reduction is up to nearly 80% in MFR1 portion, it is still not evidently sufficient to get rid of the high intensity of Cube texture from the initial fully recrystallisation. One of the incredibly convincing factors can be attributed to the feigning characteristics from the high symmetry of this orientation [45].

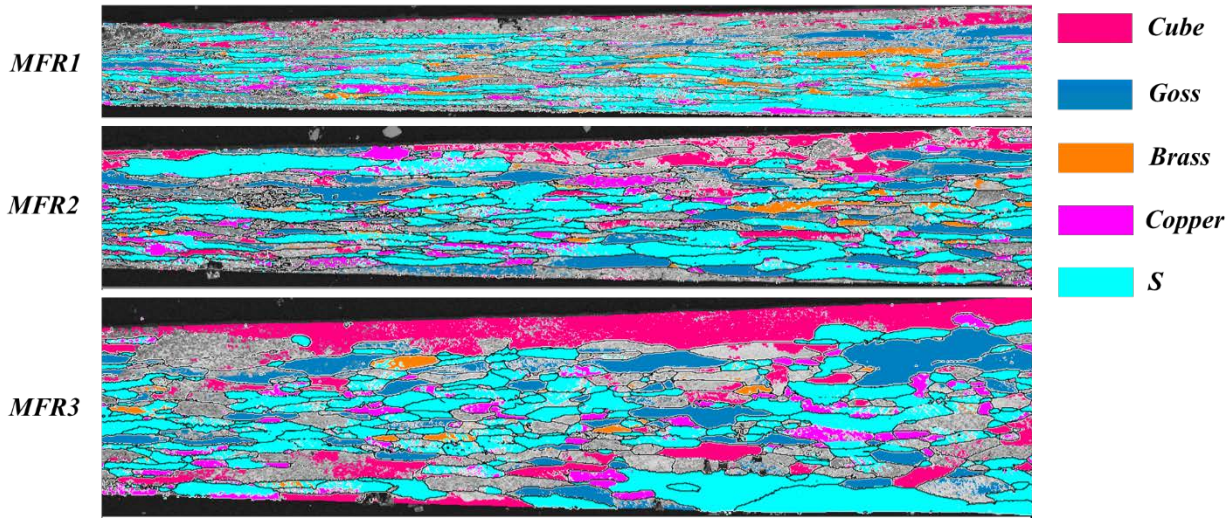

Fig. 18. Orientation distribution in three specified portions along the transition zone of micro flexibly rolled specimen.

The development of the recrystallisation textures is generally understood by two fundamental physical mechanisms which are the oriented nucleation and oriented growth theories. Although they were discussed controversially in many years, the evolution of most recrystallised textures has to be explicated using by both of them. Comprehensive investigations were made according to the evolution mechanisms of recrystallisation textures formation in various categories of commercial pure aluminium, high pure aluminium and aluminium alloys [46-50]. According to their studies, the recrystallisation textures after annealing were governed based on the details of the deformed microstructure, recrystallisation temperature and as well as the alloying components with the specified precipitation state [51], which are (i) Cube + S and/or R {124}<211>; (ii) Goss + Q {013}<231> + P {011}<122>; (iii) the rolling texture rotated from 8 potential 40 °<111> directions; and (iv) the preserved rolling texture. Nonetheless, the types (ii), (iii) and (iv) will be together with the type (i) at most time. In the current study, the texture of thin strip with varying thicknesses after annealing at 400 °C for 30 min is similar to type (i) accompanied by certain β fibre rolling texture (iii). However, the intensities of them have dropped into a large amount especially in S orientation, which was frequently formed in the aluminium alloys with few Fe additions low to 0.007% [52]. For our study, the volume fraction of Fe has reached 0.26% which means high Fe addition will also lead to the emergence of S orientation. S orientation is rather close to the R orientation and its strength generally increased with the increasing degrees of plane strains [53]. Same to the micro flexibly rolled specimens, Cube orientation also predicts a contrary development trend to the S orientation (shown in Fig. 15b). To be noted, it is the sole orientation which presents the increasing trend at A1 and A2 portions. Dillamore et al. [54] has found that the Cube nucleus preferred to be formed in transition bands. In addition, the growth of Cube oriented grains were expected due to the 40° <111> fast growth relationship in regard to the S

orientation [55]. This gives a strong understanding for the competitive relationship between the Cube and S orientations all the time in our study.

Comparatively, volume fraction of texture variations at A3 portion (Fig. 15b) illustrates completely contrary development trend to the portions of A1 and A2. The main reason is attributed to the inhomogeneous phenomenon of the grains distribution discussed hereinbefore. For the recrystallised grains, the nucleation sites of S-orientated grains are anticipated that the area they formed are adjacent to the grain boundaries in their deformed state [56]. Furthermore, they have a growth selection on behalf of expenditure of the other competitive orientations such as the Copper and Brass orientations [57]. This suggests to explain that the grain with S orientation in A3 portion of Fig. 19 presented the extreme coarse grain size.

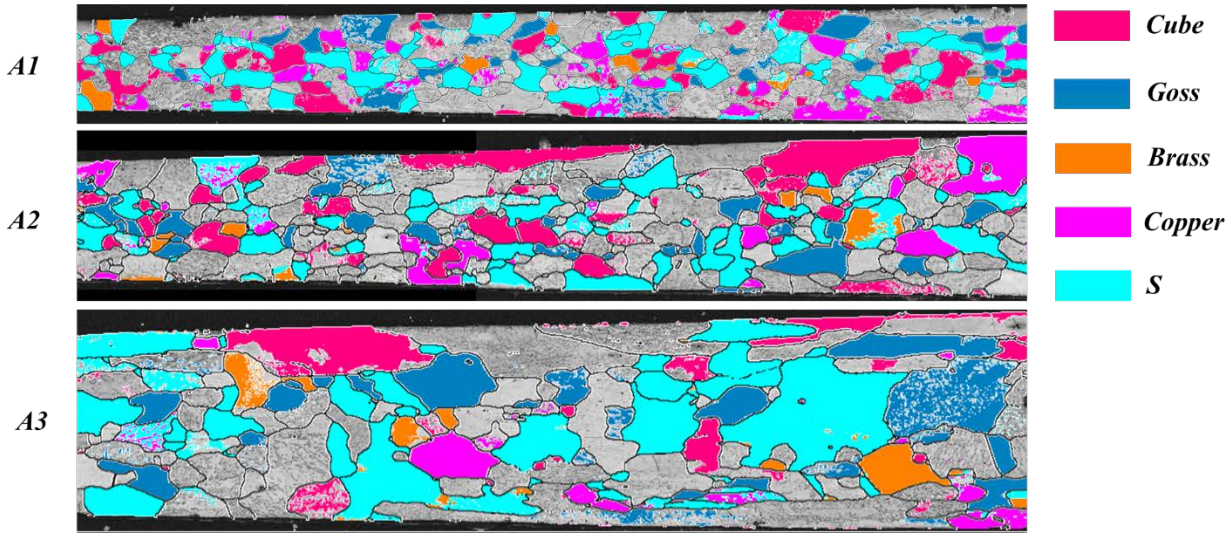

Fig. 19. Orientation distribution in three specified portions along the transition zone annealed at 400 °C for 30 min.

5 Conclusions

In this paper, the microstructure, microhardness and texture after micro flexible rolling and two kinds of subsequent annealing processes were investigated. The following conclusions are drawn:

1. The microstructure and textures of thin strip with varying thicknesses have presented clear inhomogeneous behaviour from the thicker to thinner zones in both micro flexibly rolled and annealed states.
2. Much finer grains are found in the central layer compared with those in the surface layers after recrystallisation. The resultant stress in the central layer balanced from the pressures and the frictional forces acting on the surfaces of roll bite results in relative motions, which are of importance to promote recrystallisation of finer grains.

3. Microhardness predicts work hardening or softening behaviour in the micro flexibly rolled and/or annealed strips, which is in agreement with the evolution of microstructure in the deformed or recrystallised states after rolling and/or annealing processes.
4. Development of texture in different thickness portions shows typical β fibre which shifts evidently in the longitudinal direction. Besides them, S or R orientation continually occupies the dominant rank especially in the deformed condition.

Acknowledgement

The first author gratefully appreciates UOW for PhD scholarships. This work is also supported by the grant from Australian Research Council (ARC, Grant No. FT120100432) and National Natural Science Foundation of China under Grant No. 51474127.

References

[1] U. Engel, R. Eckstein, Microforming - from basic research to its realization, Journal of Materials Processing Technology, 125 (2002) 35-44.

[2] Z. Jiang, J. Zhao, H. Xie, Microforming technology: theory, simulation and practice, (2017).

[3] J.W. Zhao, M.S. Huo, F.H. Jia, Z.Y. Jiang, Improving the Formability of Metals in Microforming, JOJ Mater Sci, 4 (2018) 555-639.

[4] L. Luo, Z. Jiang, D. Wei, X. Wang, C. Zhou, Q. Huang, Micro-hydromechanical deep drawing of metal cups with hydraulic pressure effects, Frontiers of Mechanical Engineering, 13 (2018) 66-73.

[5] H. Xie, K.-i. Manabe, T. Furushima, K. Tada, Z. Jiang, Lubrication characterisation analysis of stainless steel foil during micro rolling, Int J Adv Manuf Technol, (2015) 1-9.

[6] H.N. Lu, D.B. Wei, Z.Y. Jiang, X.H. Liu, K. Manabe, Modelling of size effects in microforming process with consideration of grained heterogeneity, Computational Materials Science, 77 (2013) 44-52.

[7] Z. Jiang, J. Zhao, H. Lu, D. Wei, K.I. Manabe, X. Zhao, X. Zhang, D. Wu, Influences of temperature and grain size on the material deformability in microforming process, Int J Mater Form, 10 (2017) 753-764.

[8] J. Zhao, H. Xie, H. Lu, Z. Jiang, Size effects in micro rolling of metals, IOP Conference Series: Materials Science and Engineering, 2017.

[9] O. Engler, C. Schäfer, H.J. Brinkman, J. Brecht, P. Beiter, K. Nijhof, Flexible rolling of aluminium alloy sheet—Process optimization and control of materials properties, Journal of Materials Processing Technology, 229 (2016) 139-148.

[10] F. Qu, Z. Jiang, D. Wei, Q. Chen, H. Lu, Study of micro flexible rolling based on grained inhomogeneity, International Journal of Mechanical Sciences, 123 (2017) 324-339.

[11] F. Qu, Z. Jiang, H. Lu, Analysis of micro flexible rolling with consideration of material heterogeneity, International Journal of Mechanical Sciences, 105 (2016) 182-190.

[12] J.X. Zhang, M. Ma, W.C. Liu, Effect of initial grain size on the recrystallization and recrystallization texture of cold-rolled AA 5182 aluminum alloy, Materials Science and Engineering: A, 690 (2017) 233-243.

[13] J. Hirsch, K. Lücke, Overview no. 76: Mechanism of deformation and development of rolling textures in polycrystalline f.c.c. metals—I. Description of rolling texture development in homogeneous CuZn alloys, Acta Metallurgica, 36 (1988) 2863-2882.

[14] I.L. Dillamore, W.T. Roberts, Rolling textures in f.c.c. and b.c.c. metals, Acta Metallurgica, 12 (1964) 281-293.

[15] M.B. Chen, J. Li, Y.M. Zhao, H. Yuan, W.C. Liu, Comparison of texture evolution between different thickness layers in cold rolled Al–Mg alloy, Materials Characterization, 62 (2011) 1188-1195.

[16] X. Wang, M. Guo, J. Luo, C. Xie, Y. Wang, J. Zhang, L. Zhuang, Effect of intermediate annealing time on microstructure, texture and mechanical properties of Al-Mg-Si-Cu alloy, Materials Characterization, 142 (2018) 309-320.

[17] H. Yuan, Q.F. Wang, J.W. Zhang, W.C. Liu, Y.K. Gao, Effect of grain shape on the texture evolution during cold rolling of Al–Mg alloys, J Alloy Compd, 509 (2011) 922-928.

[18] X.F. Wang, M.X. Guo, Y. Zhang, H. Xing, Y. Li, J.R. Luo, J.S. Zhang, L.Z. Zhuang, The dependence of microstructure, texture evolution and mechanical properties of Al–Mg–Si–Cu alloy sheet on final cold rolling deformation, J Alloy Compd, 657 (2016) 906-916.

[19] S.L. Xia, M. Ma, J.X. Zhang, W.X. Wang, W.C. Liu, Effect of heating rate on the microstructure, texture and tensile properties of continuous cast AA 5083 aluminum alloy, Materials Science and Engineering: A, 609 (2014) 168-176.

[20] X.F. Wang, M.X. Guo, L.Y. Cao, F. Wang, J.S. Zhang, L.Z. Zhuang, Effect of rolling geometry on the mechanical properties, microstructure and recrystallization texture of Al-Mg-Si alloys, International Journal of Minerals, Metallurgy and Materials, 22 (2015) 738-747.

[21] O.V. Mishin, B. Bay, G. Winther, D.J. Jensen, The effect of roll gap geometry on microstructure in cold-rolled aluminum, Acta Mater, 52 (2004) 5761-5770.

[22] C.S. Lee, F.C. Ng, K.C. Lee, The effect of rolling geometry on the distribution of deformed cube structure and its recrystallisation kinetics, Materials Science and Engineering: A, 257 (1998) 198-203.

[23] H.P. Yang, Y.H. Sha, F. Zhang, L. Zuo, Through-thickness shear strain control in cold rolled silicon steel by the coupling effect of roll gap geometry and friction, Journal of Materials Processing Technology, 210 (2010) 1545-1550.

[24] B. Major, Texture, microstructure, and stored energy inhomogeneity in cold rolled commercial purity aluminium and copper, Materials Science and Technology (United Kingdom), 8 (1992) 510-515.

[25] J.X. Zhang, C. Liu, W.C. Liu, C.S. Man, Effect of precipitation state on texture evolution in cold-rolled continuous cast AA 2037 aluminum alloy, J Alloy Compd, 728 (2017) 1199-1208.

[26] K. Lücke, O. Engler, Effects of particles on development of microstructure and texture during rolling and recrystallisation in fcc alloys, Materials Science and Technology (United Kingdom), 6 (1990) 1113-1130.

[27] O. Engler, M. Crumbach, S. Li, Alloy-dependent rolling texture simulation of aluminium alloys with a grain-interaction model, Acta Mater, 53 (2005) 2241-2257.

[28] W.C. Liu, J.G. Morris, Comparison of the texture evolution in cold rolled DC and SC AA 5182 aluminum alloys, Materials Science and Engineering: A, 339 (2003) 183-193.

[29] W.C. Liu, C.S. Man, D. Raabe, Effect of strain hardening on texture development in cold rolled Al–Mg alloy, Materials Science and Engineering: A, 527 (2010) 1249-1254.

[30] A. Rollett, F. Humphreys, G.S. Rohrer, M. Hatherly, Recrystallization and Related Annealing Phenomena: Second Edition, 2004.

[31] N. Hansen, R.F. Mehl, A. Medalist, New discoveries in deformed metals, Metallurgical and Materials Transactions A, 32 (2001) 2917-2935.

[32] B. Bay, N. Hansen, D. Kuhlmann-Wilsdorf, Microstructural evolution in rolled aluminium, Materials Science and Engineering: A, 158 (1992) 139-146.

[33] B. Bay, N. Hansen, D. Kuhlmann-Wilsdorf, Deformation structures in lightly rolled pure aluminium, Materials Science and Engineering: A, 113 (1989) 385-397.

[34] B. Bay, N. Hansen, D.A. Hughes, D. Kuhlmann-Wilsdorf, Overview no. 96 evolution of f.c.c. deformation structures in polyslip, Acta Metallurgica et Materialia, 40 (1992) 205-219.

[35] G.I. Rosen, D.J. Jensen, D.A. Hughes, N. Hansen, Microstructure and local crystallography of cold rolled aluminium, Acta Metallurgica et Materialia, 43 (1995) 2563-2579.

[36] F.J. Humphreys, A new analysis of recovery, recrystallisation, and grain growth, Mater Sci Tech-Lond, 15 (1999) 37-44.

[37] N. Hansen, Cold deformation microstructures, Materials Science and Technology (United Kingdom), 6 (1990) 1039-1047.

[38] D. Juul Jensen, N. Hansen, Flow stress anisotropy in aluminium, Acta Metallurgica et Materialia, 38 (1990) 1369-1380.

[39] L. Zhen, J. Chen, S. Yang, W. Shao, S. Dai, Development of microstructures and texture during cold rolling in AA 7055 aluminum alloy, Materials Science and Engineering: A, 504 (2009) 55-63.

[40] O. Engler, J. Hirsch, K. Lücke, Texture development in Al 1.8wt% Cu depending on the precipitation state—I. Rolling textures, Acta Metallurgica, 37 (1989) 2743-2753.

[41] X. Liu, Q. Zhao, L. Liu, Recent development on theory and application of variable gauge rolling, a review, Acta Metallurgica Sinica (English Letters), 27 (2014) 483-493.

[42] M. Huo, J. Zhao, H. Xie, Z. Jiang, Analysis of contact mechanics in micro flexible rolling, Procedia Manufacturing, 15 (2018) 1467-1474.

[43] H.-C. Kim, C.-G. Kang, M.-Y. Huh, O. Engler, Effect of primary recrystallization texture on abnormal grain growth in an aluminum alloy, Scripta Mater, 57 (2007) 325-327.

[44] O. Engler, J. Hirsch, Texture control by thermomechanical processing of AA6xxx Al–Mg–Si sheet alloys for automotive applications—a review, Materials Science and Engineering: A, 336 (2002) 249-262.

[45] O. Engler, V. Randle, Introduction to Texture Analysis: Macrotexture, Microtexture, and Orientation Mapping, Second Edition, CRC Press, 2009.

[46] I.L. Dillamore, Factors affecting the rolling recrystallisation textures in F.C.C. metals, Acta Metallurgica, 12 (1964) 1005-1014.

[47] J. Hjelen, R. Ørsund, E. Nes, On the origin of recrystallization textures in aluminium, Acta Metallurgica et Materialia, 39 (1991) 1377-1404.

[48] Z. Guo, G. Zhao, X.G. Chen, Effects of homogenization treatment on recrystallization behavior of 7150 aluminum sheet during post-rolling annealing, Materials Characterization, 114 (2016) 79-87.

[49] W. Wang, A.-L. Helbert, T. Baudin, F. Brisset, R. Penelle, Reinforcement of the Cube texture during recrystallization of a 1050 aluminum alloy partially recrystallized and 10% cold-rolled, Materials Characterization, 64 (2012) 1-7.

[50] Z.J. Wang, M. Ma, Z.X. Qiu, J.X. Zhang, W.C. Liu, Microstructure, texture and mechanical properties of AA 1060 aluminum alloy processed by cryogenic accumulative roll bonding, Materials Characterization, 139 (2018) 269-278.

[51] O. Engler, K. Lücke, Mechanisms of recrystallization texture formation in aluminium alloys, Scripta Metallurgica et Materialia, 27 (1992) 1527-1532.

[52] K. Ito, R. Musick, K. Lücke, The influence of iron content and annealing temperature on the recrystallization textures of high-purity aluminium-iron alloys, Acta Metallurgica, 31 (1983) 2137-2149.

[53] H. Ahlborn, E. Hornbogen, U. Köster, Recrystallisation mechanism and annealing texture in aluminium-copper alloys, J Mater Sci, 4 (1969) 944-950.

[54] I.L. Dillamore, H. Katoh, Mechanisms of recrystallization in cubic metals with particular reference to their orientation-dependence, Met Sci J, 8 (1974) 73-83.

[55] J.J. Sidor, R.H. Petrov, L.A.I. Kestens, Microstructural and texture changes in severely deformed aluminum alloys, Materials Characterization, 62 (2011) 228-236.

[56] O. Engler, On the origin of the R orientation in the recrystallization textures of aluminum alloys, Metallurgical and Materials Transactions A, 30 (1999) 1517-1527.

[57] O. Engler, On the influence of orientation pinning on growth selection of recrystallisation, Acta Mater, 46 (1998) 1555-1568.